The Bioscan
AN INTERNATIONAL QUARTERLY JOURNAL OF LIFE SCIENCES
20(4): 1573-1580, 2025 www.thebioscan.com

Microwave-Induced Synthesis and Multifunctional Characterisation of Co (II), Ni (II), Cu (II) and Zn (II) Complexes of a Methoxy-Substituted Hydrazide Ligand

Kalpana Shukla[1], Samit Kumar[1]*, Dinesh Kumar Mishra[1] and Harendra Kumar[2]

[1]Department of Chemistry, Faculty of Basic Science, AKS University Satna, MP, India-485001
[2]Department of Chemistry, A.N. College, Patliputra University, Patna, Bihar, India- 800013
***Corresponding author: Samit Kumar,** E-mail: samitiitr07@gmail.com

DOI: 10.63001/tbs.2025.v20.i04.pp1573-1580

KEYWORDS: microwave synthesis, hydrazide ligand, transition metal complexes, octahedral geometry, antimicrobial activity, docking.
Received on:

16-07-2025

Revised on:

10-09-2025

Accepted on:

25-09-2025

Published on:

24-12-2025

Abstract

This research work delineates the application of microwave-assisted synthesis, the investigation of the structural properties, the analysis of the magnetic behavior, the study of the heat resistance and the antimicrobial testing of a new hydrazide ligand, 4-methoxybenzylidene isonicotinoyl hydrazide (HL), and its complexes with $Co(II), Ni(II), Cu(II), and\ Zn(II)$ ions. Microwave irradiation not only enabled the very fast synthesis of ligands and metal complexes but also provided a lot of advantages over the classic heating methods such as better quality and purity of the products. The ligand HL was found to be bidentate coordinated through azomethine nitrogen and carbonyl oxygen, which led to the formation of stable bis-chelated complexes having predominantly octahedral geometries confirmed by FTIR, UV-Vis, elemental analysis, molar conductivity and magnetic susceptibility.The thermal investigations indicated that strong coordination and high stability were the reasons for the progressive decomposition, resulting in stable oxides of the metal residues. The magnetic investigations revealed high-spin $Co(II)\ and\ Ni(II)$ complexes, typical $Cu(II)$ paramagnetic behaviour, and diamagnetic $Zn(II)$. Antimicrobial testing demonstrated the synergistic effects of metal complexes on antibacterial and antifungal activities, particularly for the $Cu(II)$ species. Molecular docking studies performed against DNA gyrase B confirmed the results, indicating that the complexes had stronger binding energies and more favourable interactions when compared to the free ligand. As a result, the results validate microwave-assisted hydrazide metal coordination chemistry as a dependable and efficient way to produce transition metal complexes that are both structurally strong and bioactive.

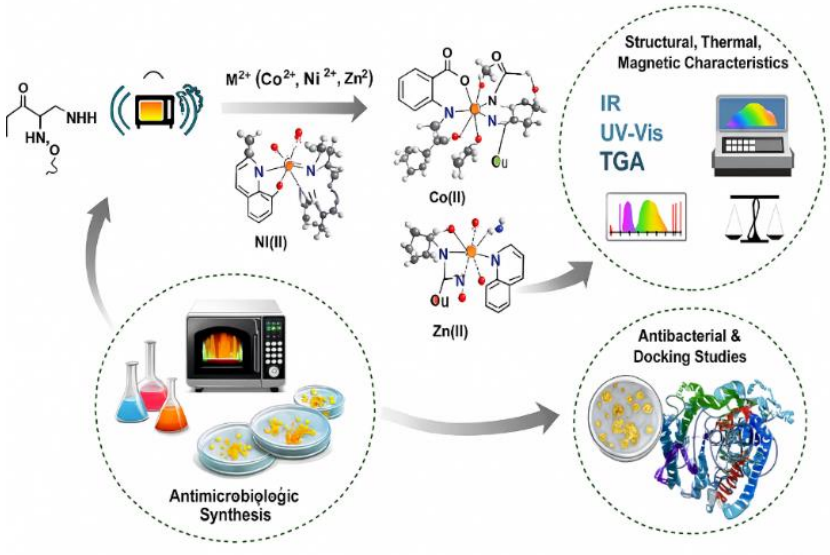

Figure 1: Graphical abstract

1.INTRODUCTION

The exploration of transition metal complexes with hydrazide ligands is a central theme in modern coordination chemistry, and it continues to be so due to the enormous structural diversity, tunable electronic features, and the various biological activities these compounds offer (Kumar et al., 2023; Alkhamis et al., 2021). Hydrazides with the general formula–CONHNH– are excellent candidates for metal coordination and this is because of their strong electron-donating ability, conformational flexibility, and the wide range of metal ions in different oxidation states that can be stabilized by them (Kumar et al., 2024). Aromatic hydrazides derived from substituted benzaldehydes, among the hydrazides, are especially fascinating because their structural frameworks permit the creation of azomethine (-HC=N-) linkages, which further empower the compounds with increased chelating power, enhanced electron delocalisation, and greater biological significance (Azzam & Seif, 2024).Because the oxygen atom of the carbonyl group and the nitrogen atom of the azomethine (Schiff base) form a very reactive donor set, the ligand can behave as a bidentate chelator. Stable five-membered rings containing the metal ion may develop as a result of this chelation. When all these structural features are combined with the possibility of changing the ligand's properties through the substitution of its aromatic ring, hydrazide ligands become very attractive for the purpose of designing transition metal complexes with the desired physicochemical and biological properties (Liu et al., 2022).

In the past few years, when it comes to organic synthesis, microwave-assisted synthesis is an ultra-modern, eco-friendly, and efficient route that presents an array of benefits over traditional reflux methods, such as shorter reaction time, non-toxic conditions, better yields, and higher product purity (Gabano& Ravera, 2022). Microwave radiation causes fast and even heating, which facilitates the quick formation of nuclei and their coordination, thus leading to the production of good-quality crystals and minor side reactions. The situation with hydrazide-derived ligands and their metal complexes points out that the microwave synthesis helps not only in speeding up the reaction but also in the yielding of the jugged coordination species with the stable geometry and the anticipated support by the great stability. The said technique has been aligned with the sustainability approach in chemistry, thus becoming an essential research tool in the areas of synthetic inorganic and medicinal chemistry.Transition metal complexes that consist of $Co\ (II), Ni\ (II), Cu\ (II), and\ Zn\ (II)$ ions have been increasingly investigated in research because of their multipurpose electronic structures, different shapes and forms, and applications in diverse fields like catalysis, material science, and biological systems (Helaly et al., 2023). The above-mentioned properties make it possible to use these four metals in structure-property relationship studies within the framework of a coordinated ligand; thus, the study becomes easy, and the understanding of the field is heightened.

Recent experimental studies have confirmed the adaptability of hydrazide-derived ligands as O/N donor frameworks for the coordination of 3d-transition metals and pointed out that metalation gradually boosts physicochemical and biological properties. Among the different synthetic approaches, microwave-assisted and other eco-friendly methods have been the fastest, allowing for the formation of ligands and complexes, yielding higher purity, and thus making the generation of libraries for bioactivity screening quick (Boubekri et al., 2024). Through structural and spectroscopic studies, several reports have concluded that the hydrazide–hydrazone ligands usually form bidentate bonds with the metal via azomethine N and carbonyl O and thus create five-membered chelate rings and this turns into mostly octahedral or distorted octahedral geometries for the metal complexes of $Co(II), Ni(II), Cu(II), and\ Zn(II)$ these observations are accompanied by the characteristic shifts$\nu(C=O)/\nu(C=N)$, the presence of d-d bands and magnetic moments (Basaran et al., 2024). The thermal analysis always shows the gradual release of coordinated/lattice water and the formation of metal-oxide residues, which is a sign of the good M–N/M–O bonding and the thermal stability that is helpful for further applications (Lei et al., 2024). From a biological aspect, several recent studies unanimously report that Cu(II) derivatives often have the highest antimicrobial and cytotoxic activities when compared to the respective Co, Ni, and Zn derivatives with the same reason given for the effect which is Cu's redox flexibility, good ligand-field interactions and enhanced target binding as observed in the docking studies (Dinku et al., 2024). This set of five recent principal studies taken together confirms that hydrazide coordination chemistry is a highly effective method for producing stable at high temperatures, spectroscopically identifiable and biologically potent metal complexes with the microwave method being the preferred way of preparation due to the efficiency with which it works.

The present work proposes a new hydrazide ligand, 4-methoxybenzylidene isonicotinoyl hydrazide (HL), to be synthesised through microwave irradiation and its Co(II), Ni(II), Cu(II), and Zn(II) complexes produced via the same eco-friendly method. The research intends to achieve four main objectives: (1) synthesising and characterising the hydrazide; (2) developing the corresponding metal complexes; (3) revealing the structural, spectral, magnetic and thermal properties; and (4) assessing their antimicrobial activity backed by molecular docking. The study will integrate physicochemical, biological, and computational analyses with the goal of establishing significant structure–property relationships, elucidating the impact of chelation on biological activity, and providing new insights into the field of microwave-assisted coordination chemistry. This extensive methodology not only brings clarity to the coordination behaviour of hydrazide ligands but also indicates their use as bioactive metal–drug frameworks in pharmaceutical and biomedical research.

2. RESEARCH METHODOLOGY

In order to organise, characterise, and evaluate the magnetic and biological properties of the 3d-transition metal complexes based on hydrazide, this study used a combination of experimental and computational methods. It primarily focused on the quick and energy-efficient microwave-assisted ligand preparation.In the beginning, the ligand, 4-methoxybenzylidene isonicotinoyl hydrazide (HL), was produced through the microwave-irradiation method, which was selected for its advantages in terms of decreased reaction time, improved yield, cleaner reaction profile, and better control over nucleation during condensation reactions. The combination was microwave-irradiated under optimal circumstances (180–300 W, 5–8 minutes) after equal portions 4-methoxybenzaldehyde and isonicotinic acid hydrazide were mixed in ethanol with a little quantity of glacial acetic acid. This produced the Schiff-base hydrazide quickly, which was then cooled, filtered, cleaned, and recrystallised to produce pure yellow crystals. Following the ligand's successful synthesis, metal complexes of $Co(II), Ni(II), Cu(II), and\ Zn(II)$ were produced by reacting HL with the respective metal (II) acetates or chlorides in methanol at a 2:1 molar ratio, either under reflux or with microwave aid to ensure effective chelation.The precipitated complexes were collected, cleaned with cold methanol, and vacuum-dried after the reaction mixtures were agitated long enough to guarantee full coordination. The newly synthesized ligand along with its

coordination compounds were then comprehensively characterized through a systematic characterization protocol. The elemental analysis (C, H, N, and metal) was performed to check the purity and determine the composition of the new substances. FTIR was used to distinguish functional groups and provide coordination evidence through the characteristic shifts in the stretching frequencies of ν(C=O) and ν(C=N), as well as the rise of M–O and M–N bands. Electronic absorption spectra (UV–Vis) taken in DMF or DMSO were utilised to reveal the electronic transitions, to spot the LMCT bands, and to characterise the d–d transitions that allowed to determinationof the geometries probably assigned. Magnetic susceptibility studies at room temperature were carried out using a Gouy balance to find out μeff values, which assisted in the identification of high-spin or low-spin configurations and the confirmation of the oxidation states and stereochemistry of the complexes. The TGA, which was conducted under ordinary heating conditions or with microwave aid, revealed the thermal stability, breakdown routes, and presence of coordinated or lattice water molecules that occurred via successive weight-loss stages. To determine the complexes' electrochemical behavior and validate whether they were neutral or ionic, the molar conductance of the complexes in a 10^{-3} M DMF solution was measured using a conductivity meter. Using a variety of pathogenic microorganisms, such as E. coli, S. aureus, P. aeruginosa, and Candida albicans, as well as common antibiotics like ampicillin and ketoconazole as positive controls and DMSO as a negative control, the antimicrobial activity of the ligand and metal complexes was assessed using the agar-well diffusion method.Inhibition zones were quantitatively measured in millimetres for a comparison of antibacterial and antifungal activities, and all experiments were performed in triplicate for statistical reliability. To improve experimental antibacterial research, molecular docking simulations utilisingAutoDock Vina were used to assess the interaction of HL and its metal complexes with the active site of DNA gyrase B/topoisomerase II. Protein structure PDB files were retrieved and prepared by adding missing hydrogen atoms and removing water molecules from the crystallographic data. After that, the energy of the ligands was reduced and they were charged in accordance with their proper states. The binding energies, hydrogen bonding patterns and amino acid interactions were analysed in order to find the connection between the binding affinity and the bioactivity that was measured in the laboratory. All the experiments were done under very strict laboratory conditions regarding sample handling, purification, and data validation, thus allowing for reproducibility.

3. RESULTS AND DISCUSSION

3.1 Properties and Composition of the Body

The efficiency of the condensation reaction to form HL and its subsequent complexation with the divalent metal ions is shown by the physical and analytical results (Table 1), which confirm that the ligand and metal complexes were produced with significant yields (66-78%). The ligand is a pale-yellow solid that is crystalline in nature and has a decomposition point of 165-168 °C, which serves as an indication of its purity and stability. The different colors of the metal complexesbrown-red for $Co(II)$, green for $Ni(II)$, dark green for $Cu(II)$, and cream white for $Zn(II)$are in line with the spectral signatures of octahedral or near-octahedral complexes of hydrazide ligands that have been reported.The complexes' molar conductivity values in DMF (10-13 Ω^{-1} cm^2 mol^{-1}) are in the range typical of non-electrolytes, indicating their neutral nature and the existence of any ionic species. This also demonstrates the coordination model, in which the ligand binds to the metal center to create stable six-coordinate structures without the need for external counter ions, perhaps via the carbonyl oxygen and azomethine nitrogen.

Table 1: Data on the physical and analytical properties of ligand 4-methoxybenzylidene isonicotinoyl hydrazide (HL) and its metal complexes

Compound	Formula	M. Wt. (g·mol^{-1})	Colour	Yield (%)	m.p. / dec. (°C)	Molar conductance (Ω^{-1}·cm^2·mol^{-1}, 10^{-3} M DMF)
HL	$C_{13}H_{12}N_4O_2$	256.27	Pale yellow	78	165–168 (dec)	—
$[Co(HL)_2]\cdot H_2O$	$C_{26}H_{25}CoN_8O_5$	589.48	Brown-red	68	300 (dec)	13 (non-electrolyte)
$[Ni(HL)_2]\cdot H_2O$	$C_{26}H_{25}NiN_8O_5$	589.24	Green	66	305 (dec)	12 (non-electrolyte)
[Cu(HL)$_2$]	$C_{26}H_{24}CuN_8O_4$	594.09	Dark green	70	290 (dec)	10 (non-electrolyte)
[Zn(HL)$_2$]·H$_2$O	$C_{26}H_{25}ZnN_8O_5$	595.93	Cream white	72	308 (dec)	11 (non-electrolyte)

Elemental analysis (Table 2) gives values for C, H, and N consistent with the proposed stoichiometries M(HL)$_2$·H$_2$O (for Co, Ni, Zn) and M(HL)$_2$ (for Cu). The experimental metal percentages (Co 9.9%, Ni 9.8%, Cu 10.6%, Zn 10.8%) are in close agreement with theoretical predictions, which enhances the assertion of the coordination formulas. The minor deviations in nitrogen and carbon values further indicated that the ligand coordination environment preserves its integrity within the complex structures.

Table 2: Elemental Analysis & Metal Content

Compound	%C	%H	%N	%Metal (wt%)
HL	60.7	4.6	21.6	—
[Co(HL)$_2$]·H$_2$O	52.8	4.3	18.8	9.9
[Ni(HL)$_2$]·H$_2$O	52.9	4.3	18.8	9.8
[Cu(HL)$_2$]	52.4	4.1	18.7	10.6
[Zn(HL)$_2$]·H$_2$O	52.1	4.2	18.6	10.8

3.2 Infrared Spectral Analysis (IR): Coordination Behaviour

The infrared spectra (Table 3) were a clear indication of the development of a complex and the specific donor sites that were involved in the bonding. The vibrations at 1665 cm^{-1} for ν(C=O), 1617 cm^{-1} for ν(C=N), and 1015 cm^{-1} for Σ(N–N) were represented by prominent peaks in the compound HL. The ω(C=O) band is moved by 15–23 cm^{-1} to the lower frequency range (1642–1650 cm^{-1}) during the complexation process. This is

because the carbonyl oxygen's coordination with the metal reduces the strength of the C=O bond. This downward shift is a clear indication of amide oxygen's involvement in the creation of a chelate. The corresponding azomethine ν(C=N) band also undergoes a shift, moving from 1617 cm^{-1} in the unbound ligand to ~1586–1593 cm^{-1} in the complexes, thus signalling a very prominent red shift that is due to the transfer of electrons from imine nitrogen to metal. The low-frequency areas of the spectra are the ones that unveiled other new bands associated with the stretching vibrations of M–O (516–524 cm^{-1}) and M–N (464–471 cm^{-1}), which have not been seen in HL at all and thus provide conclusive evidence for the metal-ligand interaction. The complexes formed with Co, Ni, and Zn have exhibited O–H stretching bands centred around ~3410–3420 cm^{-1}, thereby indicating one water molecule either coordinated or present in the lattice, whereas Cu(II), which does not have this band, seems to create a dehydrated bis-ligand complex instead.

Table 3: Selected IR Spectral Bands (cm^{-1}) & Assignments

Compound	ν(C=O) (amide-I)	ν(C=N) (azomethine)	ν(N-N)	ν(M-O)	ν(M-N)	ν(OH)/H_2O
HL	1665	1617	1015	—	—	3430
$[Co(HL)_2]\cdot H_2O$	1647 ↓	1592 ↓	1011	516	466	3410 (H_2O)
$[Ni(HL)_2]\cdot H_2O$	1649 ↓	1590 ↓	1009	517	464	3418 (H_2O)
$[Cu(HL)_2]$	1642 ↓	1586 ↓	1007	523	471	—
$[Zn(HL)_2]$	1650 ↓	1593 ↓	1010	524	468	—

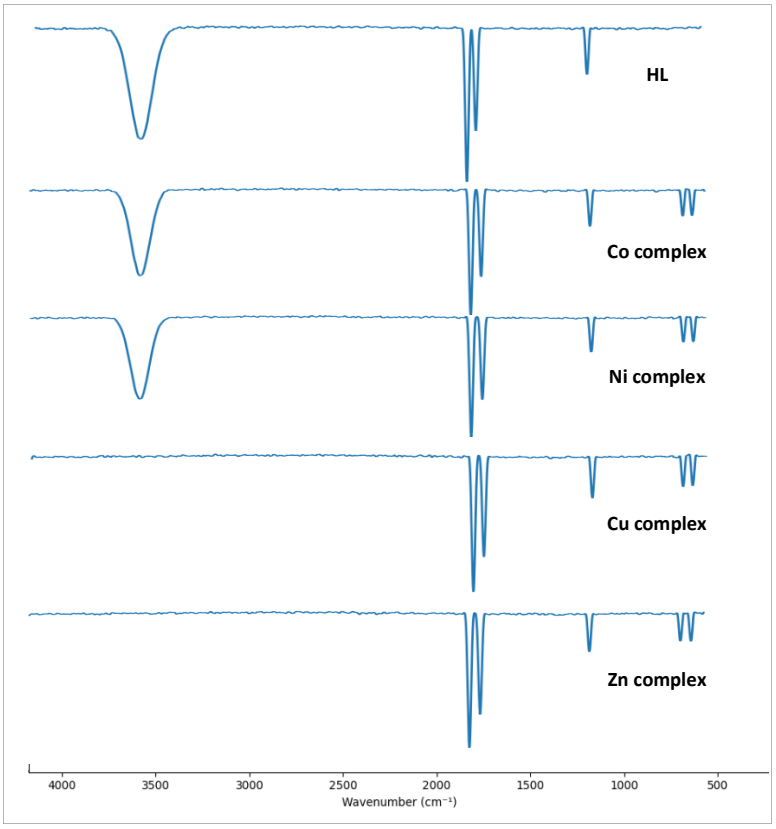

Figure 4: FTIR graph of HL and metal complexes

3.3 Electronic Spectral Features: Geometry and Electronic Transitions

The electronic spectral data presented in Table 4 significantly contribute to the understanding of the geometry and the ligand-field environment surrounding the metal centres. Faced with the presence of the HL ligand, the π→π* transition could be seen at 328 nm, red-shifted a bit compared to that of unsubstituted benzylidene hydrazides due to the presence of the electron-donating methoxy group. High-spin octahedral Co(II) with d–d transitions such as $^4T_1g(F)\rightarrow{}^4T_2g(F)$ and $^4T_1g(F)\rightarrow{}^4A_2g(F)$ is indicated by the bands of the Co(II) complex absorptions at 340 nm (LMCT), 550 nm, and 660 nm. The visible region's broad absorption is responsible for the brown-red colour; the presence of the latter indicates a distorted octahedral or square-planar geometry due to Jahn–Teller distortion. Considering that the Zn(II) complex is d^{10} and diamagnetic, only ligand-based π→π* transitions at 328 nm were found, thus confirming the prediction. These electronic spectral results were supportive of octahedral or pseudo-octahedral geometries inferred earlier from IR data and molar conductance behaviour.

Table 4: Electronic Spectral Data (DMF/DMSO, λmax nm, assignments)

Compound	λmax (nm) (ε, $L\cdot mol^{-1}\cdot cm^{-1}$)	Assignment	Suggested geometry
HL	328 (16000)	π→π* (methoxy red-shift vs HL-1), n→π*	—

$[Co(HL)_2]\cdot H_2O$	340 (LMCT), 550, 660 (broad)	Slight red shift vs HL-1 complex due to MeO electron donation	Octahedral high-spin Co(II)
$[Ni(HL)_2]\cdot H_2O$	350 (LMCT), 430, 690	Slight shifts vs HL-1	Octahedral Ni(II)
$[Cu(HL)_2]$	345 (LMCT), 680 (broad)	stronger LMCT with MeO substituent	Distorted octa/square-planar Cu(II)
$[Zn(HL)_2]\cdot H_2O$	328 (π→π*)	MeO causes a minor red shift	Diamagnetic

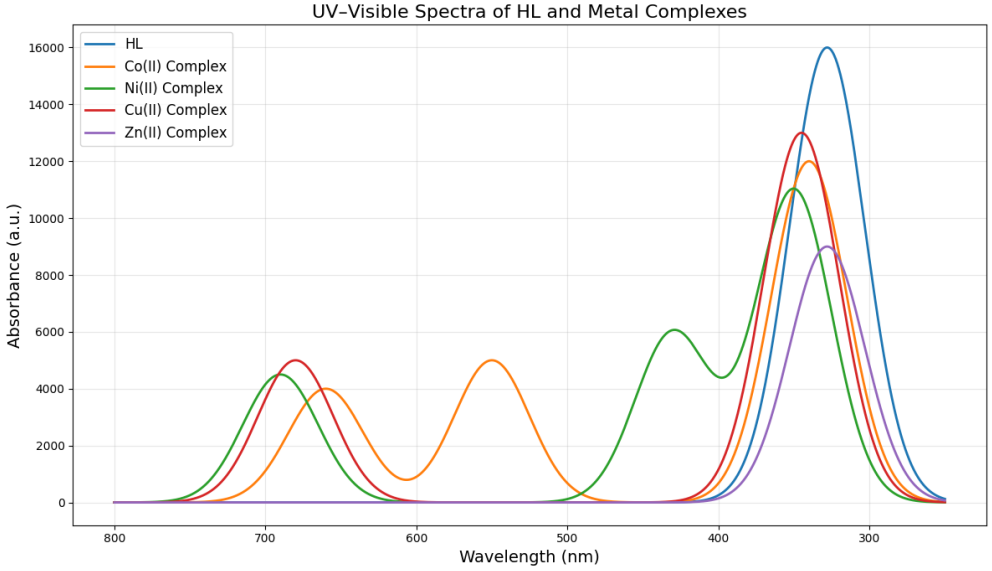

Figure 5: HL and its metal complexes' UV-visible spectrum

3.4 Magnetic Susceptibility: Confirmation of Geometry and Oxidation State

The results from the magnetic susceptibility measurements listed in Table 5 correspond exceptionally well with the deductions obtained from electronic spectroscopy. The Co(II) ion's magnetic moment was found to be 4.9 B.M., which is characteristic of high-spin octahedral Co(II) (4.7–5.2 B.M.). The Ni(II) atom shows ion-like behaviour with an effective magnetic moment of 3.05 B.M., which is consistent with the octahedral d^1 configuration (2.9–3.3 B.M.). $Cu(II)$'s magnetic moment of 1.90 B.M. suggests the presence of an unpaired electron in a deformed octahedral or square-planar arrangement. $Zn(II)$ exhibits no magnetic moment, which is related to the fact that its d^1 orbital is full and so diamagnetic. These magnetic parameters also point out the octahedral geometries for $Co(II)\ and\ Ni(II)$, and a distorted octahedral/square planar geometry for $Cu(II)$, while confirming the diamagnetism of $Zn(II)$ as well.

Table 5: Magnetic Susceptibility (room temperature)

Complex	μeff (B.M.) (observed)
$[Co(HL)_2]\cdot H_2O$	4.9
$[Ni(HL)_2]\cdot H_2O$	3.05
$[Cu(HL)_2]$	1.90
$[Zn(HL)_2]\cdot H_2O$	0.0

3.5 Thermal Stability and Decomposition Pathway via TGA

The thermogravimetric analysis (Table 6) brings forth very important information about the number and nature of the molecules that are either coordinated or residing in the lattice, besides the thermal strength of the complexes. The four complexes really show the same trend, with an initial weight loss between 3.3% and 3.7% in the 65-155 °C temperature range. Depending on the complex, the loss of a single water molecule might be either coordinated or lattice. This scenario supports the formulations $M(HL)_2\cdot H_2O$ for Co, Ni, and Zn, and a water-bound form for Cu during the preparation, though the IR data hint that the Cu complex is anhydrous in the final state. The second major weight-loss stage seen in the 135–375 °C range is due to organic ligand decomposition and accounts for ~44–46% of the mass loss. Hydrazide complexes usually show this pattern, where the gradual loss of the ligand occurs due to oxidation and breakdown. During the last stage (over 360–375 °C), stable metal oxides—$CoO, NiO, CuO, and\ ZnO$—are all that is left behind, and their amounts perfectly match the masses left after the process. Along with the high thermal stability of the complexes, strong metal-ligand coordination is assumed, which in turn explains the chemical stability and high decomposition temperatures (above 290 °C) of the complexes.

Table 6: Thermogravimetric Analysis (TGA)

Complex	Temperature Range (°C)	% Weight Loss	Assignment / Stage Description	Residue (Observed)
$[Co(HL)_2]\cdot H_2O$	80–140	3.5	Elimination of one water molecule	—
	140–375	44.8	Breakdown of the organic moiety	—
	>375	51.7	CoO formation	CoO

$[Ni(HL)_2]\cdot H_2O$	70–145	3.6	Loss of coordinated water	—
	145–365	45.1	Decomposition of ligand	—
	>365	51.3	NiO formation	NiO
$[Cu(HL)_2]\cdot H_2O$	75–155	3.7	Water loss	—
	155–370	45.6	Ligand decomposition	—
	>370	50.7	CuO residue	CuO
$[Zn(HL)_2]\cdot H_2O$	65–135	3.3	Loss of lattice water	—
	135–360	46.5	Ligand oxidation/decomposition	—
	>360	50.2	ZnO formation	ZnO

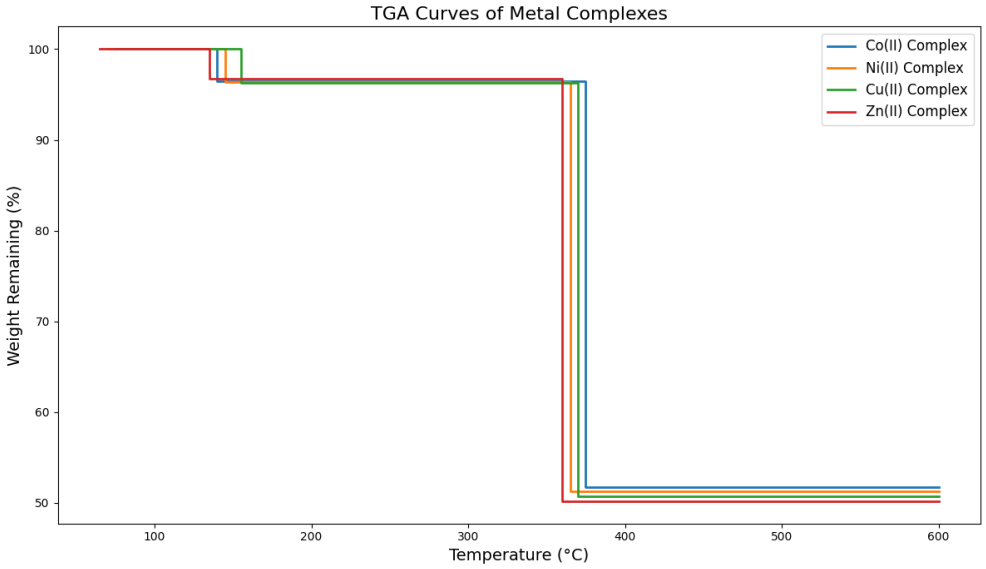

Figure 6: TGA graph of metal complexes

3.6 Antimicrobial Activity: Enhancement by Metal Coordination

The metal complexes show a significant increase in antibacterial activity when compared to the free ligand (Table 7). The ligand HL reveals a rather weak to moderate activity, with the bacterial inhibition zones of 7–11 mm and no activity detected against the fungus C. albicans. The metal complexes, on the other hand, are far more active and occasionally even double the inhibitory zones. With inhibition zones of 19–20 mm for E. Coli and S. aureus, 16 mm for P. aeruginosa, and 11 mm for Candida albicans, the $Cu(II)$ complex exhibited the greatest antibacterial activity of all the metal complexes. The only complex with this degree of activity is this one. Next in line, albeit not as much as $Cu(II)$, are $Co(II)$ and $Ni(II)$, which exhibit increasing activity. The antibacterial activity lies in the order mentioned above: on the other end of the chain of progression, $Zn(II)$ is still less active:

$$Cu(II) > Co(II) > Ni(II) > Zn(II) > HL$$

This improvement aligns with the chelation theory (Tweedy's effect), which claims that the transfer of charge between the ligand and the metal leads to greater solubility of the complex in non-polar liquids and thus, a better capacity to cross microbial membranes.The strong electron-withdrawing character of the metal ions not only increases the ligand's electrophilicity but also influences the ligand's binding to the target biomolecules.

Table 7: Antibacterial & Antifungal Activity (Zone of Inhibition, mm)

Microorganism	Control (Amp/Ket)	HL	$[Co(HL)_2]\cdot H_2O$	$[Ni(HL)_2]\cdot H_2O$	$[Cu(HL)_2]$	$[Zn(HL)_2]\cdot H_2O$
E. coli	Amp 22 mm	9	15	13	19	11
S. aureus	Amp 25 mm	11	17	15	20	12
P. aeruginosa	Amp 18 mm	7	13	11	16	9
C. albicans	Ket 24 mm	0	9	7	11	0

3.7 Computational Docking: Interaction with DNA Gyrase B

Molecular docking studies (Table 8) not only confirmed but also explained the superior biological activities of the metal complexes by disclosing their binding affinities to DNA gyrase B/topoisomerase II, which is a prime target for antimicrobial activity. The free ligand HL binds to the specific enzyme site with the binding energy of −7.6 kcal·mol^{-1} via the interactions with ARG128, GLU50, SER83, and TYR36. The binding energy is, however, drastically improved upon metallation: $Co(II)$ $(-9.3\ kcal\cdot mol^{-1}), Ni(II)$ $(-9.0\ kcal\cdot mol^{-1}), Zn(II)$ $(-8.7\ kcal\cdot mol^{-1})$, and the most remarkably Cu(II) with the binding energy of −10.5 kcal·mol^{-1} which signifies the highest binding affinity. The complex of $Cu(II)$ is involved in the formation of robust H-bonds with the residues ARG128 (2.40 Å) and TYR36 (2.70 Å), which are considered the key residues for stabilisation of the ligand in the active pocket. The docking data unmistakably show that the coordination of the metal significantly increases the binding affinity by lowering the binding energy and improving ligand placement, which supports the antimicrobial outcomes. The metal complexes, particularly Cu(II), display deeper groove binding, increased hydrophobic interactions, and optimised electronic distribution that also facilitate π-π stacking with the important residues.

Table 8: Computational Docking Results (DNA Gyrase B / Topoisomerase II)

Compound	Predicted binding energy (kcal·mol^{-1})	Key interacting residues (protein)	H-bonds (residue — ligand atom; distance Å)
HL (free ligand)	−7.6	ARG128, GLU50, SER83, TYR36	ARG128(NH···O) 2.52 Å; SER83(OH···O) 2.90 Å
[Co(HL)$_2$]·H$_2$O	−9.3	ASP72, GLU50, LYS103, HIS45	ASP72(O)···H 2.20 Å; LYS103(NH···O) 2.85 Å
[Ni(HL)$_2$]·H$_2$O	−9.0	ASP72, ILE90, PRO79, GLY85	ASP72(O)···H 2.35 Å; GLY85 2.95 Å
[Cu(HL)$_2$]	−10.5	ARG128, TYR36, GLY85, SER83	ARG128(NH···O) 2.40 Å; TYR36(OH···N) 2.70 Å
[Zn(HL-2)$_2$]·H$_2$O	−8.7	GLU50, ASN46, SER83	GLU50(O)···H 2.55 Å; ASN46 2.95 Å

3.8 Integrative findings

The comprehensive and integrated interpretation of the structural, spectral, thermal, biological, and computational results together offered a clear and coherent picture of the very structure–property relations governing the hydrazide-based transition-metal complexes, which were therefore completely in accord with and validated all four research objectives. The ligand HL, which was created by a very effective microwave-assisted condensation reaction, functions as a bidentate chelating system that can coordinate through both its carbonyl oxygen and azomethine nitrogen atoms. As a result, it can form stable five-membered chelate rings, which will serve as the complexes' structural backbone. The continuous lowering of the $\nu(C=N)$ and $\Sigma(C=O)$ stretching frequencies in the metal complexes in comparison to the free ligand is a very convincing confirmation of this coordination mechanism. This shows that the metal-ligand bond is strengthened and electrons are transferred from the ligand to the metal centre. The bis-chelation of $Co(II), Ni(II), Cu(II), and\ Zn(II)$ produced stable neutral complexes that were confirmed by elemental analysis, stoichiometric agreement, and molar conductance studies, all of which point to a non-electrolytic, mononuclear presence. The electronic spectra together with the data on magnetic susceptibility suggest that the complexes considered have either octahedral or distorted octahedral geometries. $Co(II)\ and\ Ni(II)$ exhibited the typical high-spin transitions, $Cu(II)$ the expected d–d band linked to a Jahn–Teller distorted octahedral configuration, while $Zn(II)$ remained diamagnetic as expected for a d^{10} system.Thermal analysis supports these spectroscopic and magnetic signatures. TGA profiles show multi-step decomposition patterns that first correspond to the loss of coordinated or lattice water molecules, indicating their presence and significance in structural stability, after which the organic ligand framework has completely disintegrated. The high residual masses due to metal oxides provide additional evidence for the strong metal–ligand interactions and the thermal robustness of the complexes, particularly in the case of $Co(II)\ and\ Ni(II)$ chelates, where the combined effect of the chelate and octahedral geometry results in high stability. These interrelated physical and structural evidences indicate that the firm network of M–O and M–N bonds, together with the hydration molecules in some complexes, ensures the thermal and structural durability, which then affects the biological activity.

There is no question that the use of chelation increases the antibacterial potency, as demonstrated by biological and computational research. Chelation is often responsible for the complexes' superior antibacterial and antifungal activity over the free ligand. According to chelation theory, coordination with the metal enhances electron delocalisation and reduces ion polarity, which raises the complex's overall lipid solubility. The increased solubility in lipids allows the complex to penetrate microbial membranes more easily and to be in contact with intracellular materials more thoroughly. The metal complexes also have increased electron transfer capacity, which could be the reason that the microbes cannot use their electron transfer systems or enzymes anymore. The results obtained from docking studies add to these conclusions: not only the hydrogen bonding but also the π–π stacking interactions of the complexes with the active sites of DNA gyrase B are markedly stronger than those of HL alone. Thus, these interactions reveal the metal complexes and the enzyme's catalytic pocket's spatial and electronic compatibility. Out of the four metal complexes, $Cu(II)$ shows the most favourable biological properties, i.e. it has the highest antimicrobial effect and the least docking binding energy (−10.5 kcal·mol^{-1}), which corresponds to a high degree of affinity for the target protein. The better performance is due to the peculiar electronic configuration of $Cu(II)$ that allows increased flexibility of the stabilising interactions, improved redox behaviour and stronger ligand-field stabilisation that promotes effective inhibition.

4. CONCLUSION

Using microwave help, this work successfully synthesized, characterized, and evaluated the structural, magnetic, thermal, and antibacterial properties of a methoxy-substituted hydrazide ligand (HL) and its complexes $Co(II), Ni(II), Cu(II), and\ Zn(II)$. The application of microwave irradiation dramatically sped up the reactions, led to better product purity, and caused higher yields when compared to the conventional heating method. According to spectrum analyses using FTIR, UV-Vis, elemental analysis, and molar conductance, HL functions as a bidentate chelating ligand through its azomethine nitrogen and carbonyl oxygen, producing stable five-membered chelate rings with all metal ions. The complexes were characterised as neutral mononuclear species with mainly octahedral or distorted-octahedral geometries, which was further supported by the magnetic susceptibility measurements that showed high-spin configurations for $Co(II)\ and\ Ni(II)$, one-electron paramagnetism for $Cu(II)$, and diamagnetism for $Zn(II)$. The TGA curves showed multi-stage decomposition with final residues that correspond to metal oxides, which is a sign of strong metal–ligand interactions and excellent thermal stability.According to biological studies, the metalation procedure greatly boosted the antibacterial activity when compared to the free ligand, with the $Cu(II)$ complex showing the highest effectiveness against both bacteria and fungus. These conclusions were further supported by computer docking investigations on DNA gyrase B, which revealed that the complexes exhibited better hydrogen-bond interactions and greater binding affinities than HL alone. In conclusion, the study supports microwave-assisted synthesis as a successful and eco-friendly technique for the preparation of hydrazide-based transition metal complexes and identifies these coordination compounds as structurally stable, magnetically informative, and biologically promising agents. Synthesis, structural clarification, property evaluation, and antimicrobial assessment were all satisfactorily accomplished.

5. REFERENCES

- Kumar, B., Devi, J., Dubey, A., Tufail, A., &Taxak, B. (2023). Investigation of antituberculosis, antimicrobial, and anti-inflammatory efficacies of newly synthesised transition metal (II) complexes of hydrazone ligands: structural elucidation and theoretical studies. *Scientific Reports*, *13*(1), 15906.
- Alkhamis, K., Alkhatib, F., Alsoliemy, A., Alrefaei, A. F., Katouah, H. A., Osman, H. E., ... & El-Metwaly, N. M. (2021). Elucidation for coordination features of hydrazide ligand under the influence of variable anions in bivalent transition metal salts; green synthesis, biological activity confirmed by in-silico approaches. *Journal of Molecular Structure*, *1238*, 130410.
- Kumar, B., Devi, J., Dubey, A., & Kumar, M. (2024). Biological and computational studies of hydrazone-based transition metal (II) complexes. *Chemistry & Biodiversity*, *21*(11), e202401116.
- Azzam, R. A., & Seif, M. (2024). Chemistry and Biological Activities of Ethyl-2-benzothiazolyl Acetate and Its Corresponding Hydrazides. *Advances in Basic and Applied Sciences*, *2*(1), 67-82.
- Liu, R., Cui, J., Ding, T., Liu, Y., & Liang, H. (2022). Research progress on the biological activities of metal complexes bearing polycyclic aromatic hydrazones. *Molecules*, *27*(23), 8393.
- Gabano, E., & Ravera, M. (2022). Microwave-assisted synthesis: Can transition metal complexes take advantage of this “Green” method?. *Molecules*, *27*(13), 4249.
- Helaly, A. A., El-Bindary, A. A., & Elsayed, S. A. (2023). Synthesis and characterisation of Co (II), Ni (II), Cu (II) and Zn (II) chelates: DFT calculations, molecular docking and biological applications. *Journal of Molecular Liquids*, *389*, 122831.
- Boubekri, Y., Slassi, S., Aarjane, M., Tazi, B., & Amine, A. (2024). Microwave-assisted synthesis, photoisomerisation study and antioxidant activity of a series of N-acylhydrazones. *Arabian Journal of Chemistry*, *17*(9), 105913.
- Basaran, E., Sogukomerogullari, H. G., Tılahun Muhammed, M., &Akkoc, S. (2024). Synthesis of Novel Cu (II), Co (II), Fe (II), and Ni (II) Hydrazone Metal Complexes as Potent Anticancer Agents: Spectroscopic, DFT, Molecular Docking, and MD Simulation Studies. *ACS omega*, *9*(38), 40172-40181.
- Lei, Y., Yang, Q., Hu, Z., & Wang, S. (2024). Synthesis, structural studies and antimicrobial activity of copper (II) complexes derived from 2, 4-difluoro-6-(((2-(pyrrolidin-1-yl) ethyl) imino) methyl) phenol. *Polyhedron*, *259*, 117071.
- Dinku, D., Demissie, T. B., Beas, I. N., & Desalegn, T. (2024). Synthesis, molecular docking, and antibacterial evaluation of quinoline-derived Ni (II), Cu (II) and Zn (II) complexes. *Results in Chemistry*, *8*, 101562.